



Tracking Solar Gravity Modes: The Dynamics of the Solar Core

Rafael A. García, *et al.*
Science **316**, 1591 (2007);
DOI: 10.1126/science.1140598

The following resources related to this article are available online at www.sciencemag.org (this information is current as of June 15, 2007):

Updated information and services, including high-resolution figures, can be found in the online version of this article at:

<http://www.sciencemag.org/cgi/content/full/316/5831/1591>

Supporting Online Material can be found at:

<http://www.sciencemag.org/cgi/content/full/1140598/DC1>

A list of selected additional articles on the Science Web sites **related to this article** can be found at:

<http://www.sciencemag.org/cgi/content/full/316/5831/1591#related-content>

This article **cites 24 articles**, 1 of which can be accessed for free:

<http://www.sciencemag.org/cgi/content/full/316/5831/1591#otherarticles>

This article appears in the following **subject collections**:

Astronomy

<http://www.sciencemag.org/cgi/collection/astronomy>

Information about obtaining **reprints** of this article or about obtaining **permission to reproduce this article** in whole or in part can be found at:

<http://www.sciencemag.org/about/permissions.dtl>

erochromatic genes. Based on cDNA-supported genes, it appears that euchromatin and heterochromatin genes have, on average, a similar number of exons and transcript variants per gene. In general, heterochromatic and euchromatic genes appear to encode a similar spectrum of functions, based on gene ontology (GO) analysis (Fig. 5). Some classes of genes are overrepresented in the heterochromatin, relative to the euchromatin. For example, heterochromatin genes are enriched 35-fold for putative membrane cation transporters domains (4 out of 308 heterochromatin domains versus 5 out of 13,500 euchromatin domains). Heterochromatin genes are also enriched for domains involved in DNA (53 domains) or protein binding (122 domains) that may regulate chromatin structure or function, including histone variants and proteins (Fig. 5, SOM text, and data) (11). This raises the intriguing possibility that heterochromatin may encode genes involved in its own establishment or maintenance.

Heterochromatin genes can reside in regions that approach 90% repeat content. Heterochromatin gene introns are usually composed of fragmented TE sequences (Fig. 1), are on average five times longer than euchromatin gene introns, and display less length conservation in interspecies comparisons. We found nine recursive splice site motifs nested in the long introns of heterochromatin genes, which may regulate splicing in repeat-rich regions. The underlying mechanisms that allow essential genes to be expressed and regulated in otherwise silent chromatin remain unknown. Studying heterochromatin in other species promises to shed light

on whether there are cis sequences that define or regulate boundaries between euchromatin and heterochromatin and if there are genic and non-genic regions of heterochromatin in other repeat-rich regions, including human euchromatin.

References and Notes

- R. A. Hoskins *et al.*, *Genome Biol.* **3**, RESEARCH0085 (2002).
- The Arabidopsis Genome Initiative, *Nature* **408**, 796 (2000).
- B. A. Sullivan, M. D. Blower, G. H. Karpen, *Nat. Rev. Genet.* **2**, 584 (2001).
- J. Brennecke *et al.*, *Cell* **128**, 1089 (2007).
- S. C. Elgin, S. I. Grewal, *Curr. Biol.* **13**, R895 (2003).
- E. S. Lander *et al.*, *Nature* **409**, 860 (2001).
- J. C. Venter *et al.*, *Science* **291**, 1304 (2001).
- H. R. Carlson Jr., *et al.* (www.fruitfly.org/sequence/release5genomic.shtml) (2006).
- R. Hoskins *et al.*, *Science* **316**, 1625 (2007).
- Materials and methods are available as supporting material on Science Online.
- Supplemental data can be downloaded from [ftp://ftp.dhgp.org/pub/DHGP/Science_2007_Supplemental_Data](http://ftp.dhgp.org/pub/DHGP/Science_2007_Supplemental_Data). Future updates will be released through www.flybase.net.
- C. D. Smith *et al.*, *Gene* **389**, 1 (2007).
- G. Benson, *Nucleic Acids Res.* **27**, 573 (1999).
- M. Hild *et al.*, *Genome Biol.* **5**, R3 (2003).
- Berkeley Drosophila Genome Project, www.fruitfly.org/
- K. Koczyński *et al.*, www.ncbi.nlm.nih.gov/entrez/viewer.fcgi?db=nucleotide&val=59874298.
- K. P. O'Brien, M. Remm, E. L. Sonnhammer, *Nucleic Acids Res.* **33**, D476 (2005).
- K. J. Peterson *et al.*, *Proc. Natl. Acad. Sci. U.S.A.* **101**, 6536 (2004).
- S. Foret, R. Maleszka, *Genome Res.* **16**, 1404 (2006).
- H. M. Robertson, K. W. Wanner, *Genome Res.* **16**, 1395 (2006).
- Assembly, Alignment, and Annotation of Drosophilid Genomes, http://rana.lbl.gov/drosophila/wiki/index.php/Main_Page.
- A. M. Reugels, R. Kurek, U. Lammermann, H. Bunemann, *Genetics* **154**, 759 (2000).
- J. M. Burnette, E. Miyamoto-Sato, M. A. Schaub, J. Conklin, A. J. Lopez, *Genetics* **170**, 661 (2005).
- J. R. Manak *et al.*, *Nat. Genet.* **38**, 1151 (2006).
- P. M. Harrison, D. Milburn, Z. Zhang, P. Bertone, M. Gerstein, *Nucleic Acids Res.* **31**, 1033 (2003).
- D. Torrents, M. Suyama, E. Zdobnov, P. Bork, *Genome Res.* **13**, 2559 (2003).
- R. A. Drysdale, M. A. Crosby, *Nucleic Acids Res.* **33**, D390 (2005).
- A. F. A. Smit, R. Hubley, P. Green, RepeatMasker Open-3.0, www.repeatmasker.org/.
- G. Benson, *Nucleic Acids Res.* **27**, 573 (1999).
- J. S. Kaminker *et al.*, *Genome Biol.* **3**, RESEARCH0084 (2002).
- H. Quesneville *et al.*, *PLoS Comput. Biol.* **1**, e22 (2005).
- C. M. Bergman, H. Quesneville, D. Anxolabehere, M. Ashburner, *Genome Biol.* **7**, R112 (2006).
- E. E. Slawson *et al.*, *Genome Biol.* **7**, R15 (2006).
- FlyBase, www.flybase.net/.
- GenBank, www.ncbi.nlm.nih.gov/.
- S. E. Lewis *et al.*, *Genome Biol.* **3**, RESEARCH0082 (2002).
- We thank E. Frise for maintaining the hardware and software used in these studies; M. Yandell for providing the specialized comparative genomics library-based software used in our analyses; A. Dernburg, D. Acevedo, J. Carlson, S. Celniker, R. Hoskins, and C. Kennedy for their helpful comments on the manuscript and input on annotations; and the members of the BDGP for cDNA sequencing. This work was supported by the National Human Genome Research Institute grant R01-HG000747 to C.D.S. and G.H.K. and NIH grant U54 HG004028-01 to S.S. and C.J.M.

Supporting Online Material

www.sciencemag.org/cgi/content/full/316/5831/1586/DC1

Materials and Methods

SOM Text

SOM Tables (D to F, I, and J)

References

11 January 2007; accepted 7 May 2007

10.1126/science.1139815

REPORTS

Tracking Solar Gravity Modes: The Dynamics of the Solar Core

Rafael A. García,^{1,2*} Sylvaine Turck-Chièze,^{1,2} Sebastian J. Jiménez-Reyes,³ Jérôme Ballot,^{2,4} Pere L. Pallé,³ Antonio Eff-Darwich,^{3,5} Savita Mathur,^{1,2} Janine Provost⁶

Solar gravity modes have been actively sought because they directly probe the solar core (below 0.2 solar radius), but they have not been conclusively detected in the Sun because of their small surface amplitudes. Using data from the Global Oscillation at Low Frequency instrument, we detected a periodic structure in agreement with the period separation predicted by the theory for gravity dipole modes. When studied in relation to simulations including the best physics of the Sun determined through the acoustic modes, such a structure favors a faster rotation rate in the core than in the rest of the radiative zone.

Heliology reveals the solar interior through surface observations of oscillation modes propagating inside the Sun (1, 2). Pressure-driven modes (p modes) provide a very detailed picture of the solar interior (3). Measurements of the position of the base of the convective zone (4) and the helium abundance (5) are some examples of the results achieved by the study of such modes. The structural in-

versions of the precise p-mode frequencies provide the stratification of crucial variables, such as the sound speed down to 0.05 solar radius (R_{\odot}) (6, 7). However, p modes are less sensitive to other structural variables such as density. There is less agreement between this parameter and the models in the deepest layers of the radiative zone. Moreover, the dynamical properties (8) of the solar interior (more than 60% of the total mass,

below $0.3R_{\odot}$) are not well defined. For example, large uncertainties still remain in the solar rotation profile below $0.2R_{\odot}$ (Fig. 1) because of the lack of sensitivity and the poor spatial resolution of the modes toward the deep interior (9).

To progress at greater depths and down into the solar core requires the study of another type of waves—the gravity-driven modes (g modes), for which the driving force is buoyancy. These modes are trapped within the radiative region of the Sun and become evanescent in the convective zone, reaching the solar surface with amplitudes that could be very small (10). Even considering their low surface amplitudes, g modes remain

¹DSM/DAPNIA/Service d'Astrophysique, CEA Saclay, 91191 Gif-sur-Yvette Cedex, France. ²AIM-Unité Mixte de Recherche CEA-CNRS-Université Paris VII-UMR 7158, CEA Saclay, 91191 Gif-sur-Yvette Cedex, France. ³Instituto de Astrofísica de Canarias (IAC), 38205 La Laguna, Tenerife, Spain. ⁴Max-Planck-Institut für Astrophysik, Karl-Schwarzschild-Str. 1, Postfach 1317, 85741 Garching, Germany. ⁵Departamento de Edafología y Geología, Universidad de La Laguna, Tenerife, Spain. ⁶Département Cassiopée, UMR CNRS 6202, Observatoire de la Côte d'Azur, BP 4229, 06304 Nice Cedex 4, France.

*To whom correspondence should be addressed. E-mail: rafael.garcia@cea.fr

the best probes to provide information from the solar core up to the top of the radiative region.

Solar g modes have been actively sought since 1976, without success (11). Recently, an upper limit of $\sim 1 \text{ cm s}^{-1}$ has been obtained by looking for relevant spikes in the Fourier spectrum of the observed signal above a given statistical threshold (typically 90% confidence level) and in the frequency region above $150 \mu\text{Hz}$ (12–14). A more sophisticated search of multiplets (instead of individual spikes) reduces the detection level to a few millimeters per second, yielding some g-mode candidates with a confidence level between 90% (15) and 98% (16). However, some ambiguity still surrounds their identification (attributed to quadrupole, $\ell = 2$, modes). Some scenarios have been studied explaining the visible peaks, which could constrain the physics and dynamics of the solar core. Here, we looked instead for the almost constant predicted separation (ΔP_ℓ , Fig. 2) between the periods of gravity modes with the same degree ℓ and consecutive radial order n . These separations are related to the structure and dynamics of the solar core (17). Indeed, this method is extremely sensitive to the rotation rate of the inner solar layers (18).

We used almost 10 years of velocity observations (11 April 1996 to 21 October 2005) from the Global Oscillation at Low Frequency (GOLF) instrument aboard the ESA/NASA Solar and Heliospheric Observatory (SOHO) mission. SOHO is placed around the L_1 Lagrangian point, a region at 1.5 million km from Earth toward the Sun where the gravitational field between the Sun and the Earth-Moon system equilibrates the centrifugal force. This privileged position allows continuous and uninterrupted observations of the Sun, essential for helioseismology, and provides a very stable environment. The GOLF instrument is a resonant scattering spectrophotometer (19) designed to measure line-of-sight velocity displacements of the solar photosphere. The analysis of the temporal variation of the velocity (20) in Fourier space allows the determination of the solar oscillation parameters and the derivation of the properties of the solar interior (21).

From the velocity measurements, we computed the power spectral density (PSD) by means of a fast Fourier transform algorithm. To look for the periodic signature of the g modes in this PSD, we computed a second power spectrum of the PSD between 25 and $140 \mu\text{Hz}$ (22). A broad structure in the region centered at $\sim 24 \text{ min}$ appears in this power spectrum (Fig. 3). To characterize this feature, we first used two indicators: the maximum amplitude reached (6.5σ) and the average power (2.95 times the average power of the rest of the spectrum). This feature has a high signal-to-noise ratio and is a wide structure rather than a single spike. Using a Monte Carlo simulation of $N = 6 \times 10^5$ realizations (22), we estimated the probability (likelihood) of finding a similar structure, in terms of both indicators mentioned above, produced only by pure noise with the same statistical distribution as in the GOLF

data between 22 and 26 min. We found that the likelihood that this structure is not due to noise is 99.49%. Because of the finite number of realizations, there is an uncertainty of 0.13%.

The significant structure of the GOLF power spectrum reveals the existence of quasi-periodic features somewhere in the PSD. Excluding an instrumental origin or a relation with convection (22), we studied the consequences of assuming that it is produced by the asymptotic properties of the dipole ($\ell = 1$) g modes. If this is the case, the position of the periodic structure in the PSD should follow the predicted positions of the gravity modes. To check this hypothesis, we reconstructed the fitted waves in the PSD that produced the ΔP_1 peak structure found between 22 and 26 min in the power spectrum (22).

The most striking result of this work is that the reconstructed waves issued from the real GOLF data show a pattern with their maxima at positions

near those expected from solar models (Fig. 4 and fig. S7), which supports the conjecture that they are due to gravity modes. Using the previous Monte Carlo simulation, we were able to count the number of noise realizations that matched the characteristics of the structure in the GOLF power spectrum, and to show a reconstructed wave that behaves like the one expected from g modes. To do so, we correlated the reconstructed wave of a fixed solar model with the reconstructed wave of the real data as well as with the one from the Monte Carlo simulation. To be less dependent on the physics and dynamics of the model chosen, we used three different g-mode predictions from three different solar models: the seismic model (23), the standard model S (24), and the Nice standard solar model (25). We also used different scenarios for the dynamics inside the solar core. Thus, various solar core rotation rates placed at different depths in the solar core and with different rotation axis inclina-

Fig. 1. Inversion of the solar rotation rate (Ω) using modes $\ell \leq 25$ from long time series (2088 days) of GOLF (29) and Michelson Doppler Imager (MDI) (30). In the convective zone, the differential rotation rate at different colatitudes is plotted. In the radiative region, the rotation becomes rigid down to $\sim 0.3R_\odot$. The horizontal and vertical 1σ error bars progressively increase toward the core because the p modes are less and less sensitive and because fewer and fewer modes are available for the inversion at these depths. Below $0.2R_\odot$, the rotation profile is unknown.

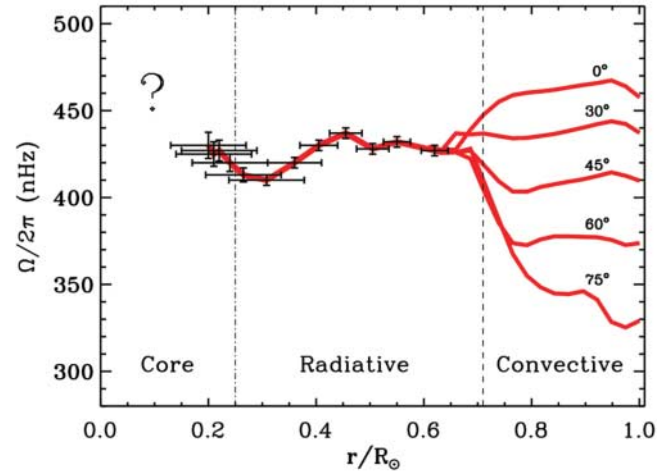
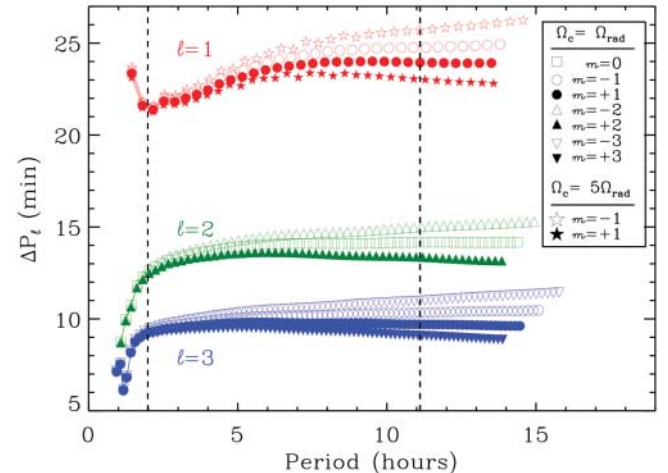


Fig. 2. Separations in period, ΔP_ℓ , between consecutive radial orders ($n, n + 1$) gravity modes for $\ell = 1, 2$, and 3 (red, green, and blue, respectively), using the theoretical frequencies from the seismic model. The constant periodicity is achieved at 6, 4, and 2 hours for the modes $\ell = 1, 2$, and 3, respectively. Ω_c is the angular velocity of the solar core, $\Omega_{\text{rad}} \approx 433 \text{ nHz}$ is the angular velocity of the remaining radiative zone, and m is azimuthal order. The star symbols show the effect, on the dipole ($\ell = 1$) modes, of an increased solar core rotation rate—up to 5 times that of the remaining radiative zone ($\Omega_c = 5\Omega_{\text{rad}}$)—below a core radius $R_c = 0.15R_\odot$. For the sake of clarity, we have not drawn the effect for higher-degree modes. Inside the zone limited by the two vertical dashed lines (from ~ 2 to ~ 14 hours, corresponding to 25 to $140 \mu\text{Hz}$), we expect periodicities between 22 and 26 min for the $\ell = 1$ mode, between 9 and 15 min for the $\ell = 2$ mode, and between 5 and 11 min for the $\ell = 3$ mode.



tions were used (22). The correlation of the reconstructed waves of these sets of models with that of the real GOLF data—in the region between 2 and 8.5 hours—always gave a correlation above 20%, with the highest values around 50%. The correlations with the Monte Carlo simulations were usually below 1%. Only 905 of the $N = 6 \times 10^5$ realizations reached 20% correlation, and only 43 of these realizations reached 50% correlation. Thus, the likelihood that this kind of periodic structure in the GOLF data is not produced by noise is at least 99.85% and can reach 99.99% in the best case (up to 4σ level of a normal distribution).

The set of parameters that characterizes the physics and dynamics inside the solar core is too large to be totally constrained by this first analysis. However, from all the sets of g-mode predictions used, we obtained better correlations with those having an inner rotation rate in the range three to five times the rest of the radiative region, this being independent of the inclination axis and the radius of the core used (better results

at $0.15R_\odot$). The correlation is higher with the model with a higher rotation rate in the core (Fig. 4). Unfortunately, the solar rotation profiles used in the simulations of the core are unrealistic (i.e., a constant rotation rate without differential rotation). On the other hand, the comparison with simulations including noise (fig. S10) tends to favor the hypothesis of a finite lifetime for the g modes, as recently suggested (26). In both cases, further studies will be necessary.

The analysis presented here shows the robust detection of a spectral feature compatible with the presence of a periodic pattern in the PSD with a confidence level above 99.49% (corresponding to more than 3σ of a normal distribution). The accurate study of this quasi-periodic pattern found in the GOLF data is compatible with the presence of gravity dipole modes with radial orders from $n = -4$ to -26 , with a confidence level above 99.85%. A detailed comparison with solar models tends to favor a faster core rotation than in the rest of the radiative zone, with a confidence level

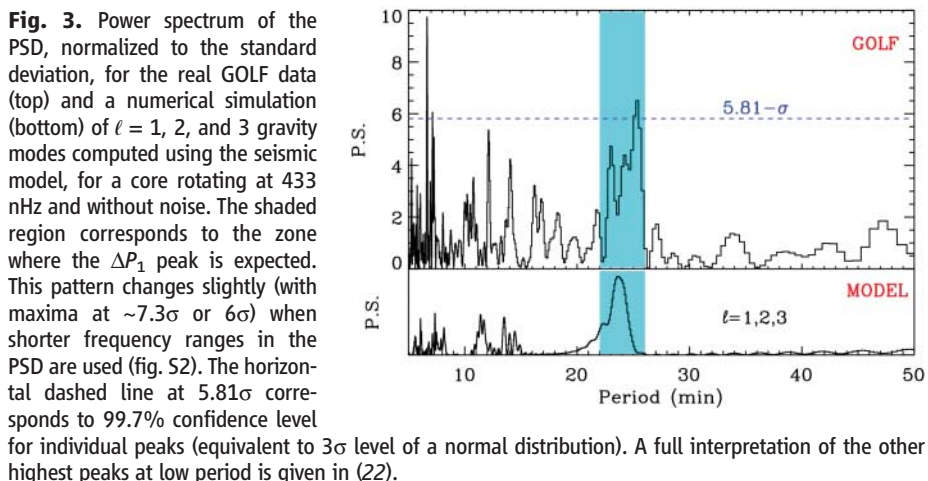


Fig. 3. Power spectrum of the PSD, normalized to the standard deviation, for the real GOLF data (top) and a numerical simulation (bottom) of $\ell = 1, 2$, and 3 gravity modes computed using the seismic model, for a core rotating at 433 nHz and without noise. The shaded region corresponds to the zone where the ΔP_1 peak is expected. This pattern changes slightly (with maxima at $\sim 7.3\sigma$ or 6σ) when shorter frequency ranges in the PSD are used (fig. S2). The horizontal dashed line at 5.81σ corresponds to 99.7% confidence level for individual peaks (equivalent to 3σ level of a normal distribution). A full interpretation of the other highest peaks at low period is given in (22).

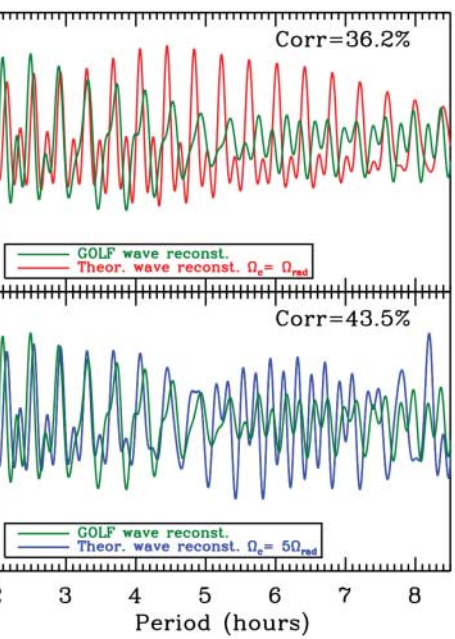


Fig. 4. Reconstructed waves in the PSD (arbitrary units) corresponding to the peak structure between 22 and 26 min in the power spectrum for the GOLF data. (Top) Comparing the theoretical reconstructed waves (red curve) with the one issued from GOLF (green curves), we first observe that the maxima match rather well the expected positions of the g modes at low periods. Moreover, the latter is wider and for periods greater than 4 hours it is divided into two waves, which suggests the presence of both m components of the $\ell = 1$ modes (higher splitting). The correlation between both reconstructed waves is 36.2%. (Bottom) The higher correlation, 43.5%, between the second model (a core rotating 5 times as fast as the radiative zone below $R_c = 0.15R_\odot$) and GOLF tends to favor a faster rotation rate in the core than in the rest of the radiative zone. As a comparison, the correlation with randomized data is below 1% (fig. S8).

above 99.99%. The detection of g-mode asymptotic properties opens the opportunity for further studies of the rotation and the magnetic field inside the deepest layers of the Sun and can stimulate further observational studies with SOHO, ground-based networks, and next-generation space missions such as Picard (27) and DynaMICCS (28).

References and Notes

1. J. Christensen-Dalsgaard, *Rev. Mod. Phys.* **74**, 1073 (2002).
2. The oscillation modes are characterized by three quantum numbers: the radial order n , the angular degree ℓ , and the azimuthal order m ($-\ell \leq m \leq \ell$).
3. D. O. Gough *et al.*, *Science* **272**, 1296 (1996).
4. J. Christensen-Dalsgaard, D. O. Gough, J. Toomre, *Science* **229**, 923 (1985).
5. S. V. Vorontsov, V. A. Baturin, A. A. Pamiatnykh, *Nature* **349**, 49 (1991).
6. S. Basu *et al.*, *Mon. Not. R. Astron. Soc.* **292**, 243 (1997).
7. S. Turck-Chièze *et al.*, *Astrophys. J.* **555**, L69 (2001).
8. M. J. Thompson *et al.*, *Science* **272**, 1300 (1996).
9. M. J. Thompson, J. Christensen-Dalsgaard, M. S. Miesch, J. Toomre, *Annu. Rev. Astron. Astrophys.* **41**, 599 (2003).
10. P. Kumar, E. J. Quataert, J. N. Bahcall, *Astrophys. J.* **458**, L83 (1996).
11. H. Hill, C. Fröhlich, M. Gabriel, V. Kotov, in *Solar Interior and Atmosphere*, A. N. Cox, W. C. Livingston, M. S. Matthews, Eds. (Univ. of Arizona Press, Tucson, AZ, 1991), p. 562.
12. T. Appourchaux *et al.*, *Astrophys. J.* **538**, 401 (2000).
13. A. H. Gabriel *et al.*, *Astron. Astrophys.* **390**, 1119 (2002).
14. W. J. Chaplin *et al.*, *Mon. Not. R. Astron. Soc.* **336**, 979 (2002).
15. S. Turck-Chièze *et al.*, *Astrophys. J.* **604**, 455 (2004).
16. S. Turck-Chièze *et al.*, in *Helio- and Astroseismology: Towards a Golden Future*, D. Danesy, Ed. (European Space Agency, Noordwijk, Netherlands, 2004), pp. 85–90.
17. S. Mathur, S. Turck-Chièze, S. Couvidat, R. A. García, in *Beyond the Spherical Sun: A New Era of Helio- and Astroseismology*, K. Fletcher, Ed. (European Space Agency, Noordwijk, Netherlands, 2006), pp. 95–98.
18. J. Provost, G. Berthomieu, *Astron. Astrophys.* **165**, 218 (1986).
19. A. H. Gabriel *et al.*, *Sol. Phys.* **162**, 61 (1995).
20. R. A. García *et al.*, *Astron. Astrophys.* **442**, 385 (2005).
21. S. Turck-Chièze *et al.*, *Solar Phys.* **175**, 247 (1997).
22. See supporting material on Science Online.
23. S. Couvidat, S. Turck-Chièze, A. G. Kosovichev, *Astrophys. J.* **599**, 1434 (2003).
24. J. Christensen-Dalsgaard *et al.*, *Science* **272**, 1286 (1996).
25. J. Provost, G. Berthomieu, P. Morel, *Astron. Astrophys.* **353**, 775 (2000).
26. B. Dintrans, A. Brandenburg, A. Nordlund, R. F. Stein, *Astron. Astrophys.* **438**, 365 (2005).
27. G. Thuillier, S. Dewitte, W. Schmutz, *Adv. Space Res.* **38**, 1792 (1991).
28. S. Turck-Chièze *et al.*, in *Trends in Space Science and Cosmic Vision 2020*, F. Favata, J. Sanz-Forcada, A. Giménez, B. Battrick, Eds. (European Space Agency, Noordwijk, Netherlands, 2005), pp. 193–203.
29. R. A. García *et al.*, *Sol. Phys.* **220**, 269 (2004).
30. S. G. Korzenik, *Astrophys. J.* **626**, 585 (2005).
31. The GOLF experiment is based on a consortium of institutes (Institut d’Astrophysique Spatiale, CEA/Saclay, Nice, and Bordeaux Observatories, France; IAC, Spain) involving a large number of scientists and engineers, as enumerated in (19). SOHO is a mission of international cooperation between ESA and NASA. This work is supported in part by Spanish MEC grant AYA2004-04462. We thank T. Appourchaux, W. J. Chaplin, and all the PHOEBUS group (22) for useful discussions and comments.

Supporting Online Material

www.sciencemag.org/cgi/content/full/1140598/DC1
Materials and Methods
Figs. S1 to S10
References

30 January 2007; accepted 19 April 2007
Published online 3 May 2007;
10.1126/science.1140598
Include this information when citing this paper.